Journal of Biomechanics 149 (2023) 111483

Contents lists available at ScienceDirect

Journal of Biomechanics

journal homepage: www.elsevier.com/locate/jbiomech

Effects of implant and vocal fold stiffness on voice production after medialization laryngoplasty in an MRI-based vocal fold model

Liang Wu [a,b], Zhaoyan Zhang [b,*]

[a] Key Laboratory of Biomedical Information Engineering of Ministry of Education, School of Life Science and Technology, Xi'an Jiaotong University, Xi'an 710049, PR China

[b] Department of Head and Neck Surgery, University of California, Los Angeles, 31-24 Rehabilitation Center, 1000 Veteran Avenue, Los Angeles, CA 90095-1794, USA

ARTICLE INFO

Keywords:
Medialization laryngoplasty
Implant stiffness
MRI-based model
Voice production
Acoustics

ABSTRACT

Medialization laryngoplasty is one of the primary surgical interventions in the treatment of glottal insufficiency due to vocal fold paralysis, paresis, or atrophy. During the surgery, an implant is laterally inserted into the larynx to medialize the affected vocal fold toward glottal midline, with the goal of improving glottal closure during phonation and voice production efficiency. While implants of different materials and geometry designs have been used, the effect of implant design on the voice outcome remains unclear. In this simulation study, the effect of implant stiffness was investigated in an MRI-based model of the vocal folds after medialization laryngoplasty. The results showed that implant stiffness had a significant impact on the phonation threshold pressure, glottal area waveform, and fundamental frequency, but only small effect on the closed quotient and other acoustic measures of the produced voice. The effect of implant stiffness also exhibited variability, depending on the stiffness conditions of the vocal fold and paraglottic tissues, indicating that individual differences need to be considered during the planning of medialization laryngoplasty.

1. Introduction

Medialization laryngoplasty is one of the primary surgical intervention procedures in the treatment of glottal insufficiency due to vocal fold paralysis, paresis, or atrophy (Isshiki, 1989; Daniero et al., 2014; Crolley and Gibbins, 2017). During the surgery, an implant is laterally inserted into the larynx to medialize the affected vocal fold toward glottal midline, with the goal of improving glottal closure during phonation and voice production efficiency (Isshiki, 1989). A variety of implants has been developed using different materials (e.g. hydroxyapatite, titanium, silicone, and Gore-tex; Storck et al., 2007; Schneider et al., 2003; van Ardenne et al., 2011; Shen et al., 2013; Suehiro et al., 2009) and with different geometry designs (e.g. Hoffman et al., 2011, 2014; Devos et al., 2010; Frizzarini et al., 2012). While medialization laryngoplasty is often effective in improving the voice outcome, for some patients, particularly professional voice users, the voice outcome may remain unsatisfactory. While an unsatisfactory voice outcome generally indicates unsuccessful restoration of vocal fold geometry and stiffness conditions required for normal voice production, the specific factors contributing to the unsatisfactory outcome are often unclear.

Many studies have investigated the effects of different implant designs (stiffness and shape) on voice outcomes after medialization laryngoplasty, often with variable or even conflicting results. For example, while Oreste et al. (2014) found that implants with a divergent medial surface shape achieved a better pressure/flow relationship under large medialization depth condition, a more recent study showed that implants with a rectangular medial surface consistently improved the cepstral peak prominence (CPP) of the produced voice (Reddy et al., 2022). No optimal medial surface shape was identified by Zhang et al. (2015), which showed that rectangular implants had large impact on fundamental frequency but nonrectangular implants were slightly better in improving high-order harmonic excitation. Furthermore, Zhang et al. observed that implant stiffness had a much larger effect on the degree of acoustic improvement than implant medial surface shape. They recommended soft implants with comparable stiffness to the vocal folds, due to the reduced sensitivity of voice outcome improvements to implant insertion depth. Similar recommendation in favor of softer implants was made by Smith et al. (2020). In contrast, the study in Reddy et al. (2022) showed that Silastic implants with a rectangular medial surface outperformed other implant design in improving CPP, although considerable variability was observed in their data. Cameron et al. further pointed out that design of implant stiffness should consider the

* Corresponding author.
E-mail address: zyzhang@ucla.edu (Z. Zhang).

https://doi.org/10.1016/j.jbiomech.2023.111483
Accepted 1 February 2023
Available online 4 February 2023
0021-9290/© 2023 Elsevier Ltd. All rights reserved.

target airflow range, because stiffer implants generally provided better acoustic improvements and more stable pressure/flow relationship at higher airflow rates (Cameron et al., 2020).

These conflicting findings likely result from the fact that implant insertion simultaneously impacts vocal fold geometry, stiffness, and position, all of which are important parameters determining voice production at the laryngeal level (Zhang, 2016a). In addition to directly modifying vocal fold position, implant properties (geometry and stiffness) and how the implant is inserted also determine the post-insertion geometry of the vocal folds, particularly the medial surface shape, which has an important role in determining voice outcomes (Zhang, 2016a,2016b,2022). Secondly, after insertion the implant occupies a large portion of the space originally occupied by the pre-insertion vocal folds, with the post-insertion vocal folds compressed into a thin layer around the implant (Zhang et al., 2020). Thus, stiffness of the implant directly determines how the combined implant-vocal fold system vibrates. Lastly, patient-specific differences in geometry and stiffness of the affected vocal folds are expected to play some role in determining voice outcomes after medialization laryngoplasty, although not much is known at the present.

Unfortunately, it is difficult to isolate these different effects of implant stiffness in animal or human models, which also do not allow control for vocal fold geometric and stiffness properties. In our previous study (Zhang et al., 2020), implant insertion and its impact on post-insertion vocal fold geometry were investigated using magnetic resonance imaging (MRI). The goal of the present study is to further understand how voice production after medialization laryngoplasty is affected by implant stiffness at different stiffness conditions of the affected vocal fold due to patient-specific differences. In order to isolate effects of implant stiffness from the effects of vocal fold stiffness, a computational model developed in our previous studies was used, which allowed us to parametrically vary implant and vocal fold stiffness one at a time and observe their impact on voice production. While imaging-based vocal fold models have been developed in previous studies (e.g., Mittal et al., 2011; Vampola et al., 2016; Wu and Zhang, 2019; Smith et al., 2020; Chen et al., 2020; Movahhedi et al., 2021; Li et al., 2021), voice production after medialization laryngoplasty has not been systematically investigated.

In this study, MRI images of larynges after medialization laryngoplasty obtained from our previous studies were used to reconstruct a three-dimensional model of the combined implant-vocal fold system, thus assuring the clinical relevance of the simulations. While the post-insertion geometry of the implant-vocal fold system is expected to vary with implant and vocal fold stiffness (Zhang et al., 2020), in this study the MRI-derived geometry was intentionally kept constant while the stiffness of the vocal fold and implant was systematically varied. This research design allows us to focus on the direct effect of changes in vocal fold and implant stiffness on voice production, and isolate this effect from voice changes associated with differences in post-insertion vocal fold geometry due to the use of implants of varying stiffness, which is difficult to achieve in human or animal models. We believe that being able to isolate these two effects of implant stiffness (direct effect of implant being an integral component of the vibrating implant-vocal fold system and the impact of implant design on post-insertion vocal fold geometry which indirectly affects phonation) is essential to understand the source of variability in voice outcomes after medialization laryngoplasty. The effect of implant design on post-insertion vocal fold geometry will be investigated in a future study.

2. Methods

2.1. MRI-based vocal fold geometry model

A three-dimensional model of the human larynx after medialization laryngoplasty was reconstructed from MRI images of an excised human larynx (age 82, female). The larynx was harvested from autopsy at the Department of Pathology, University of California, Los Angeles within 24 h postmortem. The larynx was stored at −80 °C after dissection and thawed on the day of experiment. Before MRI scanning of the larynx, medialization laryngoplasty was performed using a Silastic implant, as described in (Zhang et al., 2020). Fig. 1**a** shows the geometry of the implant which had a rectangular medial surface shape and Young's modulus of 1386 kPa. As in previous studies (Zhang et al., 2015), the superior edge of the thyroplasty window was at the level of the true vocal fold, while the inferior edge was parallel to and 2 mm from the inferior border of the thyroid cartilage. With the anterior edge placed 5 mm posterolateral to midline, the window had an approximate size of 10 mm × 5 mm.

The larynx was scanned using a Bruker BioSpec 7 Tesla MRI (Bruker Biospin GmbH, Rheinstetten, Germany) with a 30-mm inner diameter surface coil. High-quality images with a spatial resolution of 0.1 mm × 0.1 mm × 0.1 mm, as shown in Fig. 1**b**, were obtained through a standard rapid acquisition with relaxation enhancement imaging sequence. The MRI images were then segmented by the first author manually, and the implant, cartilages (including the thyroid, cricoid, and arytenoid cartilages), thyroarytenoid (TA) muscle, cover layer (the lamina propria and epithelium), and paraglottic space (including the lateral cricoarytenoid muscle and connective soft tissue) were reconstructed using a commercial software (Simpleware, Synopsys, Inc.). The boundaries of different cartilages, soft tissue layers, and muscles are color coded in Fig. 1b. A three-dimensional model of the larynx and implant was then developed from the segmentation (Wu and Zhang, 2019) using Gaussian smoothing as shown in Fig. 1**c**.

The prephonatory glottis was set to be nearly closed with a prephonatory glottal opening area of 3.3 mm^2 or a glottal angle of 0.7°, corresponding to a barely abducted glottal configuration. The left and right vocal folds were assumed to be symmetric about the glottal midline in geometry and stiffness, so only one vocal fold was considered in the simulation.

2.2. Voice production model and simulation conditions

Voice production simulations were performed as described in our previous studies (Zhang, 2015, 2017; Wu and Zhang, 2021**)**. Readers are referred to these previous studies for details of the model formulation. Based on an eigenmode-based formulation of system governing equations, this model is computationally efficient and able to reproduce experimental observations (Farahani and Zhang, 2016; Zhang and Luu, 2012). In brief, the glottal airflow is modeled as a one-dimensional quasi-steady flow with a viscous loss along the glottal channel. While the vocal folds are known to exhibit a nonlinear mechanical behavior, in this study the vocal folds are modeled as linear elastic materials, with the understanding that the elastic moduli represent tangent moduli that vary with tissue deformation. With this linear elasticity simplification, changes in vocal fold stiffness due to vocal fold deformation can then be modeled by appropriate variations in the elastic moduli of the vocal folds. Specifically, the vocal folds are modeled as a transversely isotropic, nearly incompressible, linear elastic material with an isotropic plane perpendicular to the anterior-posterior (AP) direction. The control parameters for the mechanical properties of the vocal folds include the transverse Young's modulus *Et*, AP shear modulus G_{ap}, and AP Young's modulus E_{ap}, AP Poisson's ratio $\nu_{ap} = 0.495$, and density $\rho = 1030\ kg/m^3$. As in our previous studies, $E_{ap} = 4G_{ap}$ was assumed in this study in order to reduce the number of control parameters. The implant was modeled as an isotropic linear elastic material with a Young's modulus E_{im}. The paraglottic space, which includes the lateral cricoarytenoid (LCA) muscle and connective soft tissues, was also modeled as an isotropic linear elastic material with a Young's modulus E_{pg}, as in previous study (Wu and Zhang, 2021). All cartilages were fixed in the model.

Table 1 lists the specific conditions simulated in this study. Three vocal fold stiffness conditions (L1, L2, and L3) were considered to represent individual physiological differences. For the implant, four

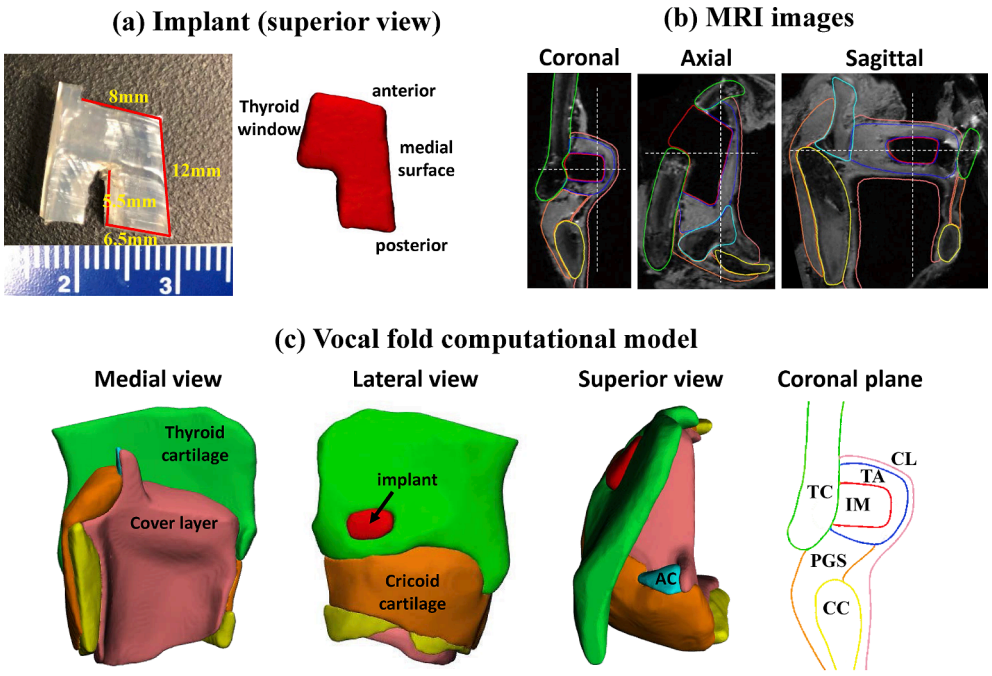

Fig. 1. MRI-based vocal fold computational model. (a) Dimension of the implant used in medialization laryngoplasty and its reconstructed geometry model. (b) Magnetic resonance images of the larynx after implant insertion and segmentation of different cartilages and muscles in three views. The dashed white lines in each view indicate the cut planes from which the other two views were generated. (c) The three-dimensional model of the vocal fold after medialization laryngoplasty reconstructed from the MRI images.

Table 1
Simulation conditions.

	L1	L2	L3
Transverse Young's modulus E_t (kPa)	1	1	2
AP shear modulus G_{ap} (kPa)	10	20	10
Implant Young's modulus E_{im} (kPa)	[5.5, 11, 22, 1386]		
Paraglottic space modulus E_{pg} (kPa)	[1, 4, 10]		
Subglottal pressure P_s (Pa)	[50, 100, 200, 300, 400, 500, 600, 700, 800, 900, 1000, 1200, 1400, 1600, 1800, 2000, 2200, 2400]		

values for E_{im} were selected according to the implant used in previous experimental studies (Orestes et al., 2014; Zhang et al., 2015; Cameron et al., 2020). Due to the lack of experimental data on the stiffness of the paraglottic space, three values of the E_{pg} were considered as in a previous study (Wu and Zhang, 2021), representing a range of paraglottic space conditions from the resting state (paralysis) to conditions of weak LCA activation (paresis or presbyphonia). For each stiffness condition, the subglottal pressure was varied in steps from 50 to 2400 Pa as in previous studies (Wu and Zhang, 2019,2021). Thus, a total of 648 simulations were performed, each simulating a 0.5-second-long sustained phonation at a sampling rate of 44,100 Hz. For each simulation, the produced sound was calculated from the airflow at the glottal exit using a monopole source model.

2.3. Data analysis

For each simulation, analysis was performed using the last 0.25-second of the voice, during which vocal fold vibration generally has reached the steady state. A typical waveform of the glottal area and glottal flow is shown in Fig. 2. Phonation threshold pressure (P_{th}) was estimated as the minimum subglottal pressure that produced sustained vocal fold vibration. The mean glottal area Ag_{mean} and glottal area amplitude Ag_{amp} (half of the peak-to-peak amplitude) were calculated from the glottal area waveform. The closed quotient CQ was calculated as the percentage of the glottal cycle that the glottal flow rate remained

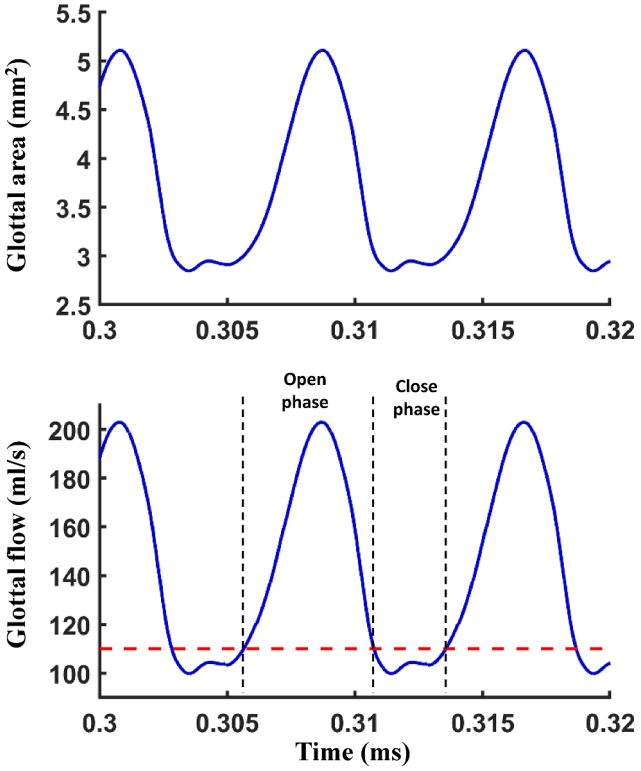

Fig. 2. Typical waveforms of glottal area and glottal flow rate under the condition with Et = 1 kPa, Gap = 10 kPa, Epg = 4 kPa, Eim = 22 kPa, and Ps = 700 Pa. In the bottom panel, the horizontal dashed line indicates the lower 10% of the glottal flow waveform, which is used to determine the open and closed phases of the glottal cycle. The closed quotient was calculated as the ratio between the closed phase and the period of the glottal cycle.

within the lowest 10% of the glottal flow waveform (Fig. 2). For voice acoustics, the fundamental frequency F_0, sound pressure level SPL, and subharmonic-to-harmonic ratio SHR (Sun, 2002) were extracted using the VoiceSauce (Shue et al., 2011).

3. Results

Fig. 3 shows the effect of implant stiffness on phonation threshold pressure (P_{th}) under different vocal fold and paraglottic conditions. Generally, the implant stiffness had a significant impact on the phonation threshold pressure, but the overall pattern of variation also depended on the stiffness condition of the vocal folds and paraglottic tissues. For example, for a paraglottic space stiffness $E_{pg} = 10$ kPa, P_{th} decreased with increasing implant stiffness for the vocal fold stiffness condition with $E_t/G_{ap} = 1/10$ kPa, but this trend was reversed for the vocal fold stiffness condition with $E_t/G_{ap} = 1/20$ kPa. Similarly, opposite effects of the implant stiffness on the P_{th} also occurred for different paraglottic space stiffness conditions. For example, for vocal fold stiffness conditions with $E_t/G_{ap} = 1/20$ kPa, the trend of variation of P_{th} with varying implant stiffness for a paraglottic stiffness $E_{pg} = 1$ kPa was opposite of that for a paraglottic stiffness $E_{pg} = 4$ kPa.

Similar variability in the effect of implant stiffness on P_{th} has been observed in previous experimental studies (Zhang et al., 2015; Cameron et al., 2020). For example, Cameron et al. showed that P_{th} decreased with increasing implant stiffness in one human larynx but increased in another (Fig. 5b in Cameron et al., 2020). Thus, our results showed that larynx-specific differences in vocal fold and paraglottic tissue stiffness are one possible source of the observed variability in how P_{th} varies with implant stiffness.

Fig. 3 also shows that this variability was larger for the stiffest and softest implants, and relatively smaller for the two intermediate implant stiffnesses ($E_{im} = 11$ and 22 kPa). In particular, conditions with $E_{im} = 22$ kPa had the lowest mean value of the P_{th} across all conditions, indicating a relatively optimal implant stiffness.

The variability in the dependence of phonation threshold pressure on implant stiffness appeared to be partially related to the ability of the vocal fold in maintaining adductory position when subject to airflow, as illustrated in Fig. 4. The figure shows the mean glottal area, glottal area amplitude, and closed quotient at different stiffness conditions and subglottal pressures. Comparison of Figs. 3 and 4 shows that for vocal fold conditions that were not able to maintain adductory position against the airflow (e.g., $E_t = 1$ kPa, $G_{ap} = 10$ kPa, $E_{pg} = 1$ kPa), as quantified by a large change in mean glottal area with varying implant stiffness in Fig. 4, P_{th} decreased with increasing implant stiffness. In contrast, when the vocal folds were able to maintain adductory position against the airflow, as quantified by a small change in mean glottal area with varying implant stiffness (e.g., $E_t = 1$ kPa, $G_{ap} = 20$ kPa, $E_{pg} = 10$ kPa), P_{th} generally increased with increasing implant stiffness. For vocal fold conditions in between (i.e, small changes in the mean glottal area with varying implant stiffness), P_{th} first decreased then increased with increasing implant stiffness. Thus, the variability in the variation of P_{th} with increasing implant stiffness in Fig. 3 appears to result from the interplay of two conflicting effects of increasing implant stiffness: while increasing implant stiffness alone increased the phonation threshold pressure, implant stiffness increase also decreased mean glottal opening area, which lowers the phonation threshold pressure.

Fig. 4 also shows that decreasing implant stiffness increased the mean glottal area, indicating that a softer implant results in a larger glottal opening. This effect was consistent across all vocal fold and paraglottic stiffness conditions but weakened with an increase in either vocal fold stiffness or paraglottic tissue stiffness. In contrast, the effect of implant stiffness on the glottal area amplitude and closed quotient were variable and inconsistent. This is confirmed in Table 2, which shows the results of multiple linear regression between selected output measures and model controls. While vocal fold stiffness had a significant effect on both the mean glottal area and glottal area amplitude, the effect on the closed quotient was statistically significant only for the AP stiffness.

The effect of vocal fold and implant stiffness on the produced voice acoustics is shown in Fig. 5 and Table 2. The fundamental frequency F_0 increased significantly with increasing longitudinal vocal fold stiffness G_{ap}, implant stiffness E_{im}, and subglottal pressure P_s. This trend indicates that stiffer implants led to a higher vocal pitch, as would be expected. Table 2 also shows that F_0 decreased slighted with increasing transverse stiffness E_t, contradicting previous findings. This was likely due to the small number of conditions with $E_t = 2$ kPa that reached sustained phonation. The sound pressure level was primarily determined by the subglottal pressure and vocal fold transverse stiffness, although a small effect of implant stiffness can be observed in Table 2. Similarly, Table 2 shows that CPP was primarily determined by the subglottal pressure in this study, and the effects of vocal fold stiffness and implant stiffness were insignificant.

Fig. 5 and Table 2 also show that for conditions with large implant stiffness, large paraglottic space stiffness, and low subglottal pressure, vocal folds were more likely to exhibit subharmonic vibration, as quantified by high SHR values. Similar observation was made in our previous study (Wu and Zhang, 2021). Note that this region of high SHR values also had relatively high values of CQ. This suggests that for vocal folds that are not completely paralyzed, use of stiff implants is more likely to result in tight glottal conditions with irregular vocal fold vibration and voice production with a rough voice quality.

4. Discussion and conclusions

The goal of this study was to investigate the effects of implant

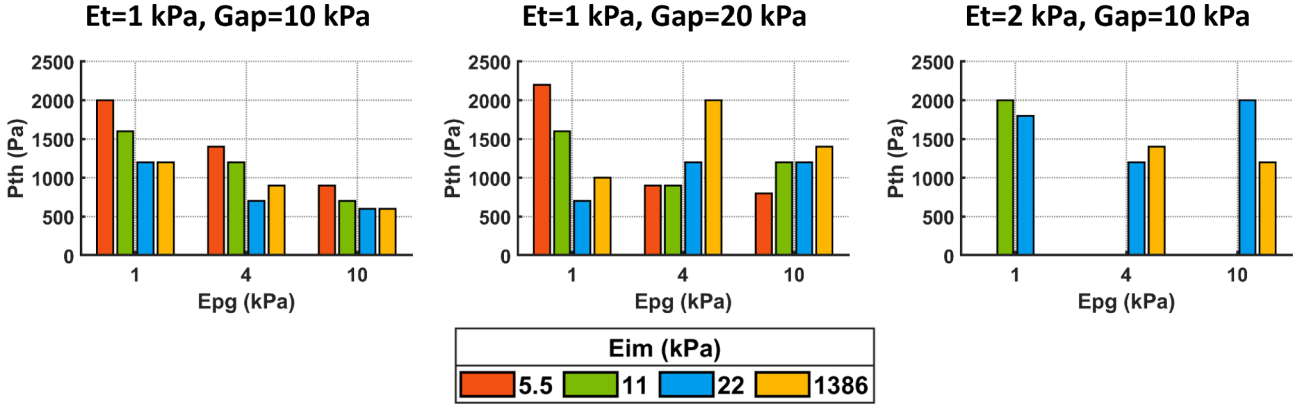

Fig. 3. Phonation threshold pressure (P_{th}) as a function of implant stiffness (E_{im}) under different vocal fold conditions (E_{pg} and E_t/G_{ap}). The missing data in the right panel indicate conditions for which no sustained phonation was observed.

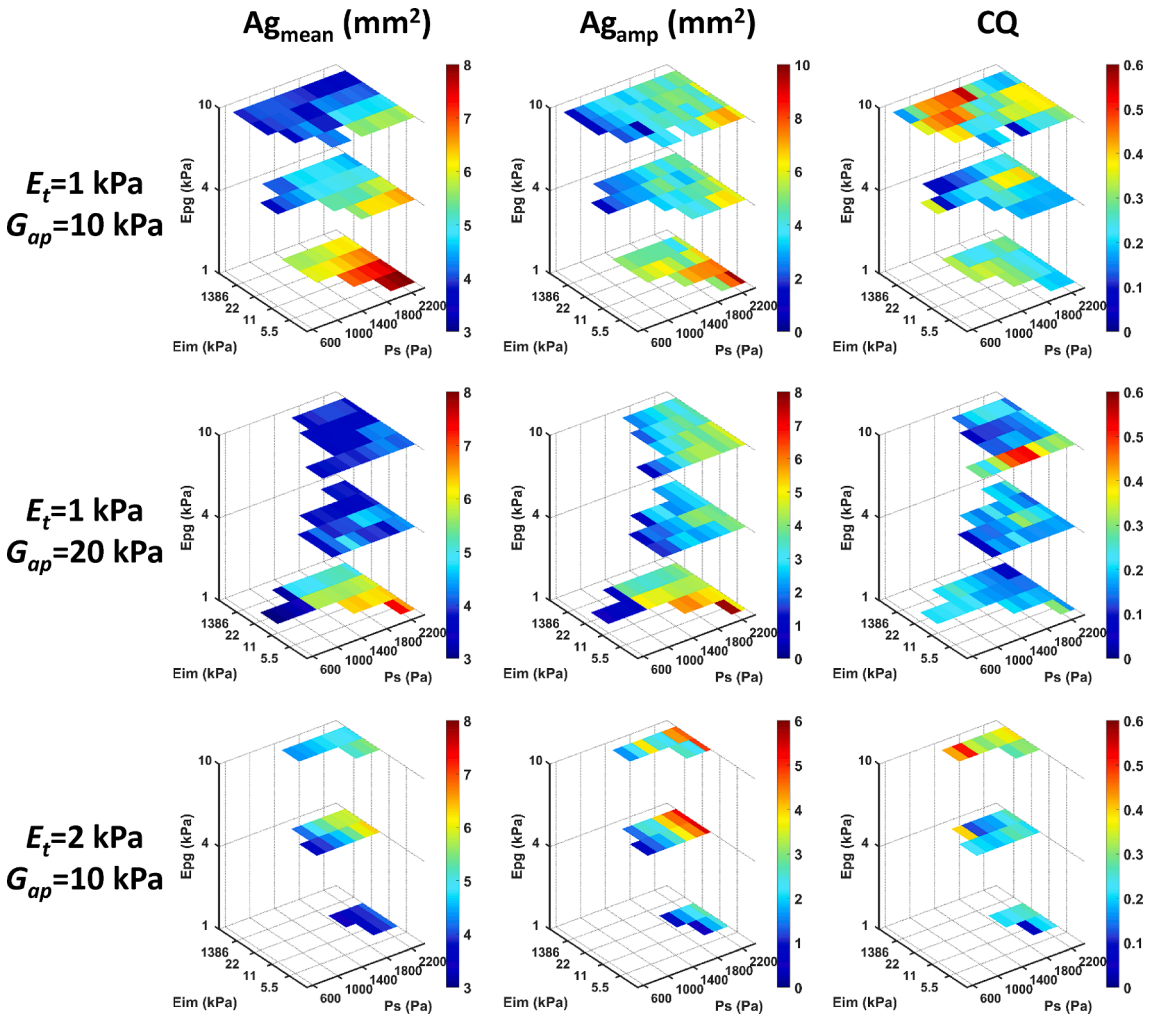

Fig. 4. Selected measures of voice production as different vocal fold and implant stiffness conditions. The measures include the mean glottal area (Ag_{mean}), glottal area amplitude (Ag_{amp}), and closed quotient (CQ). Regions without data indicate conditions of no phonation.

Table 2
Results from multiple linear regression between selected output measures and model controls and the corresponding R^2 values. Coefficients with an absolute value >0.1 are highlighted in bold. * denotes p > 0.05.

Selected measures		Ag_{mean}	Ag_{amp}	CQ	F_0	SPL	CPP	SHR
Standardized coefficients	E_t	**-0.220**	**-0.491**	0.014*	-0.084	**-0.408**	0.083*	-0.034*
	G_{ap}	**-0.428**	**-0.438**	**-0.324**	**0.578**	**-0.125**	0.003*	**0.142**
	E_{im}	**-0.101**	-0.080*	0.007*	**0.259**	0.097	0.064*	**0.142**
	E_{pg}	**-0.456**	-0.068*	**0.338**	-0.049*	**0.179**	**0.130***	0.0421
	P_s	**0.377**	**0.621**	-0.052*	**0.610**	**0.825**	**-0.258**	**-0.328**
R^2		0.513	0.573	0.248	0.782	0.692	0.099	0.367

stiffness on voice production after medialization laryngoplasty. The effects of the implant are twofold. Once inserted, the implant becomes part of the vibrating structure and thus directly impacts vocal fold vibration and voice production. In addition, implant stiffness also affects vocal fold deformation during insertion and post-insertion vocal fold geometry, particularly the medial surface shape, thus indirectly impacting voice production. In this study, using an MRI-based model of vocal folds after medialization laryngoplasty, we focused on the first effect of the implant stiffness. Our results showed that implant stiffness had important effect on the glottal area waveform, particularly the mean glottal opening, fundamental frequency of vocal fold vibration, and phonation threshold pressure. In contrast, implant stiffness had a much reduced effect on the closed quotient, glottal area amplitude, and CPP, indicating a small effect on the produced voice quality. These observations are consistent with the effects of the body-layer stiffness on voice production in a body-cover vocal fold model without implants. This is not surprising considering that by compressing and stretching the vocal folds, the implant occupies a large portion of the space of the original vocal folds (Zhang et al., 2020). In other words, the implant takes over the structural role of the body layer after implantation, except that the implant lacks the active control capability of the thyroarytenoid muscle.

Our results also showed that the effect of implant stiffness can vary significantly subject to individual differences in the stiffness conditions of the affected vocal fold and paraglottic space tissues which include connective soft tissues and lateral cricoarytenoid muscle. This was particularly the case for the effect of implant stiffness on phonation

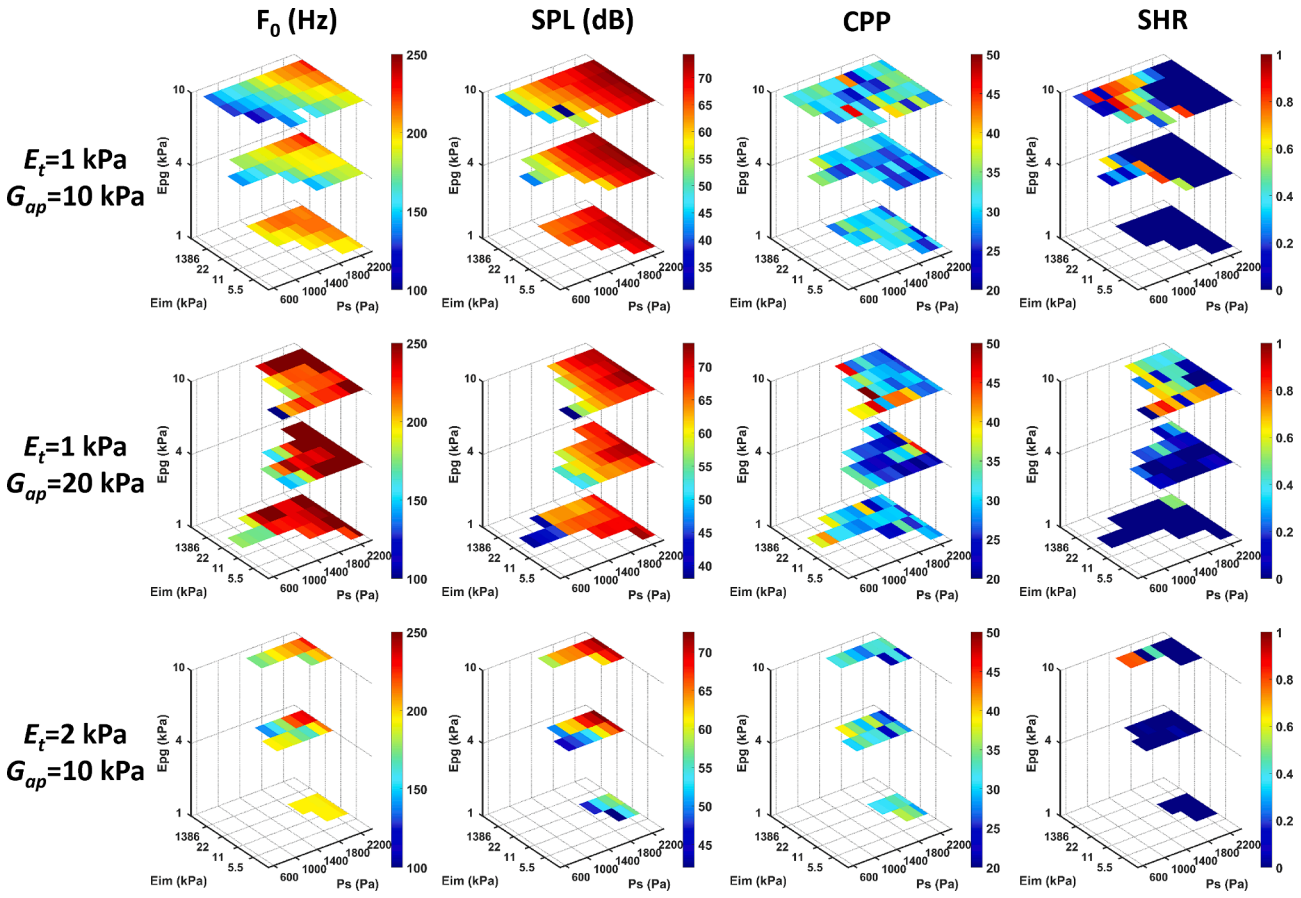

Fig. 5. Selected acoustic output measures at different vocal fold and implant conditions. See the text for the definition of the different measures. Regions without data indicate conditions of no phonation.

threshold pressure. Depending on the stiffness condition of the vocal fold and paraglottic tissues, the phonation threshold pressure may either increase, decrease, or decrease then increase with increasing implant stiffness, as observed in previous experimental studies (Zhang et al., 2015; Cameron et al., 2020). This indicates a potential role of larynx-specific differences in vocal fold stiffness in determining voice outcomes of medialization laryngoplasty, and that such differences need to be taken into consideration during the planning of medialization laryngoplasty.

Our results further showed that this variability was largely related to the implant's ability to provide lateral support to the vocal folds against the glottis-opening effect of the airflow. When the implant was too soft to provide sufficient lateral support, variations in vocal fold and paraglottic tissue stiffness had a more noticeable role in determining the mean glottal opening (Wu and Zhang, 2021) and thus the phonation threshold pressure. On the other hand, implants that were too stiff often led to a tight glottal configuration and thus irregular vibration. In our previous study (Wu and Zhang, 2021), we showed that the implant stiffness has to be higher than 10 kPa. The results in the present study showed that implants with intermediate stiffness $E_{im} = 22$ kPa had an overall low phonation onset across different vocal fold conditions. This indicates a potentially optimal implant stiffness range around 10-22 kPa.

While our results showed a small effect of implant stiffness on the closed quotient and CPP, it should be noted that the post-insertion vocal fold geometry was intentionally kept constant in this study, in order to isolate the two effects of implant stiffness on voice production, as discussed above. Previous studies showed that the medial surface shape plays a dominant role in determining the closed quotient and CPP. With the medial surface shape kept constant in our study, it is not surprising that we only observed small variations in the closed quotient and CPP. In reality, post-insertion vocal fold geometry highly depends on implant stiffness, among many other factors including surgeon experience and the biomechanical state of the vocal folds. The effect of implant stiffness on post-insertion vocal fold geometry will be investigated in future studies.

Another limitation was that only one larynx geometry derived from MRI reconstruction of a Silastic-medialized vocal fold was investigated. The implant-vocal fold deformation during implant insertion is expected to vary with implant stiffness and geometry as well as individual differences in vocal fold geometry and stiffness, which is likely to influence the impact of implant stiffness on voice production. For example, because of the relatively large vertical thickness of the post-insertion medial surface in this study, the phonation threshold pressure was relatively high, resulting in no phonation in many conditions (especially with high vocal fold stiffness like $E_t/G_{ap} = 2/10$ kPa). Generalization of the findings of this study thus requires further studies using different post-insertion vocal fold geometry from different individuals and with different implants.

Finally, a few simplifications were made in the computational model in order to achieve a computational speed required for parametric simulations as in our study. These include simplifications on both the fluid and structure sides of the model. The glottal flow was simplified to a one-dimensional quasi-steady flow with an ad-hoc flow separation model. While vocal folds are known to exhibit nonlinear mechanical behavior, in this study they were simplified as linear elastic materials. While these simplifications are often made in phonation models and our previous studies showed that the model was able to reproduce experimental observations, the findings of this study need to be verified in models in which the different physical components are more accurately represented and in well-controlled experiments.

CRediT authorship contribution statement

Liang Wu: Writing – review & editing, Writing – original draft, Visualization, Validation, Methodology, Investigation, Formal analysis, Data curation. **Zhaoyan Zhang:** Writing – review & editing, Writing – original draft, Visualization, Validation, Supervision, Software, Resources, Project administration, Methodology, Investigation, Funding acquisition, Formal analysis, Data curation, Conceptualization.

Declaration of Competing Interest

The authors declare that they have no known competing financial interests or personal relationships that could have appeared to influence the work reported in this paper.

Acknowledgments

This work was support by research grant R01DC020240 from the National Institute on Deafness and Other Communication Disorders, the National Institutes of Health.

References

Cameron, B.H., Zhang, Z., Chhetri, D.K., 2020. Effects of thyroplasty implant stiffness on glottal shape and voice acoustics. Laryngosc. Invest. Otolaryngol. 5 (1), 82–89.
Chen, Y., Li, Z., Chang, S., Rousseau, B., Luo, H., 2020. A reduced-order flow model for vocal fold vibration: from idealized to subject-specific models. J. Fluids Struct. 94, 102940.
Crolley, V., Gibbins, N., 2017. One hundred years of external approach medialisation thyroplasty. J. Laryngol. Otol. 131, 202–208.
Daniero, J., Garrett, G., Francis, D., 2014. Framework surgery for treatment of unilateral vocal fold paralysis. Curr. Otorhinolaryngol. Reports 2, 119–130.
Devos, M., Schultz, P., Guilleré, F., Debry, C., 2010. Thyroplasty for unilateral vocal fold paralysis using an adjustable implant in porous titanium. Eur. Ann. Otorhinolaryngol. Head Neck Dis. 127 (6), 204–212.
Farahani, M.H., Zhang, Z., 2016. Experimental validation of a three-dimensional reduced-order continuum model of phonation. J. Acoust. Soc. Am. 140(2), EL172–EL177.
Frizzarini, R., Gebrim, E.M., Imamura, R., Tsuji, D.H., Moyses, R.A., Sennes, L.U., 2012. Individually customized implants for laryngoplasty—are they possible? J. Voice 26 (5), 619–622.
Hoffman, M.R., Witt, R.E., McCulloch, T.M., Jiang, J.J., 2011. Preliminary investigation of adjustable balloon implant for type I thyroplasty. Laryngoscope 121 (4), 793–800.
Hoffman, M.R., Devine, E.E., McCulloch, T.M., Jiang, J.J., 2014. Excised larynx evaluation of wedge-shaped adjustable balloon implant for minimally invasive type I thyroplasty. Laryngoscope 124 (4), 942–949.
Isshiki, N., 1989. Phonosurgery: Theory and Practice. Springer-Verlag, Tokyo. Chapter 6.
Li, Z., Wilson, A., Sayce, L., Avhad, A., Rousseau, B., Luo, H., 2021. Numerical and experimental investigations on vocal fold approximation in healthy and simulated unilateral vocal fold paralysis. Appl. Sci. 11 (4), 1817.
Mittal, R., Zheng, X., Bhardwaj, R., Seo, J.H., Xue, Q., Bielamowicz, S., 2011. Toward a simulation-based tool for the treatment of vocal fold paralysis. Front. Physiol. 2, 19.
Movahhedi, M., Geng, B., Xue, Q., Zheng, X., 2021. A computational framework for patient-specific surgical planning of type 1 thyroplasty. JASA Exp. Lett. 1 (12), 125203.
Orestes, M.I., Neubauer, J., Sofer, E., Salinas, J., Chhetri, D.K., 2014. Phonatory effects of type I thyroplasty implant shape and depth of medialization in unilateral vocal fold paralysis. Laryngoscope 124 (12), 2791–2796.
Reddy, N., Lee, Y., Zhang, Z., Chhetri, D., 2022. Optimal thyroplasty implant shape and stiffness for treatment of acute unilateral vocal fold paralysis: evidence from a canine in vivo phonation model. Proc. Interspeech 2022, 2273–2277.
Schneider, B., Denk, D.M., Bigenzahn, W., 2003. Functional results after external vocal fold medialization thyroplasty with the titanium vocal fold medialization implant. Laryngoscope 113 (4), 628–634.
Shen, T., Damrose, E.J., Morzaria, S., 2013. A meta-analysis of voice outcome comparing calcium hydroxylapatite injection laryngoplasty to silicone thyroplasty. Otolaryngol. Head Neck Surg. 148 (2), 197–208.
Shue, Y.-L., Keating, P., Vicenik, C., Yu, K., 2011. VoiceSauce: a program for voice analysis, in: Proceedings of the ICPhS XVII, pp. 1846–1849.
Smith, S.L., Titze, I.R., Storck, C., Mau, T., 2020. Effect of vocal fold implant placement on depth of vibration and vocal output. Laryngoscope 130 (9), 2192–2198.
Storck, C., Brockmann, M., Schnellmann, E., Stoeckli, S., Schmid, S., 2007. Functional outcome of vocal fold medialization thyroplasty with a hydroxyapatite implant. Laryngoscope 117, 1118–1122.
Suehiro, A., Hirano, S., Kishimoto, Y., Tanaka, S., Ford, C.N., 2009. Comparative study of vocal outcomes with silicone versus Gore-Tex thyroplasty. Ann. Otol. Rhinol. Laryngol. 118 (6), 405–408.
Sun, X., 2002. Pitch determination and voice quality analysis using subharmonic-to-harmonic ratio. In: 2002 IEEE International Conference on Acoustics, Speech, and Signal Processing, vol. 1, pp. I-333–I-336. <https://doi.org/10.1109/ICASSP.2002.5743722>.
Vampola, T., Horáček, J., Klepáček, I., 2016. Computer simulation of mucosal waves on vibrating human vocal folds. Biocybernet. Biomed. Eng. 36 (3), 451–465.
Van Ardenne, N., Vanderwegen, J., Van Nuffelen, G., De Bodt, M., Van de Heyning, P., 2011. Medialization thyroplasty: vocal outcome of silicone and titanium implant. Eur. Arch. Otorhinolaryngol. 268 (1), 101–107.
Wu, L., Zhang, Z., 2019. Voice production in a MRI-based subject-specific vocal fold model with parametrically controlled medial surface shape. J. Acoust. Soc. Am. 146 (6), 4190–4198.
Wu, L., Zhang, Z., 2021. Impact of the paraglottic space on voice production in an MRI-based vocal fold model. J. Voice. https://doi.org/10.1016/j.jvoice.2021.02.021.
Zhang, Z., 2015. Regulation of glottal closure and airflow in a three-dimensional phonation model: Implications for vocal intensity control. J. Acoust. Soc. Am. 137 (2), 898–910.
Zhang, Z., 2016a. Mechanics of human voice production and control. J. Acoust. Soc. Am. 140 (4), 2614–2635.
Zhang, Z., 2016b. Cause-effect relationship between vocal fold physiology and voice production in a three-dimensional phonation model. J. Acoust. Soc. Am. 139 (4), 1493–1507.
Zhang, Z., 2017. Effect of vocal fold stiffness on voice production in a three-dimensional body-cover phonation model. J. Acoust. Soc. Am. 142 (4), 2311–2321.
Zhang, Z., 2022. Contribution of undesired medial surface shape to suboptimal voice outcome after medialization laryngoplasty. J. Voice. https://doi.org/10.1016/j.jvoice.2022.03.010.
Zhang, Z., Chhetri, D.K., Bergeron, J.L., 2015. Effects of implant stiffness, shape, and medialization depth on the acoustic outcomes of medialization laryngoplasty. J. Voice 29 (2), 230–235.
Zhang, Z., Luu, T., 2012. Asymmetric vibration in a two-layer vocal fold model with left-right stiffness asymmetry: experiment and simulation. J. Acoust. Soc. Am. 132 (3), 1626–1635.
Zhang, Z., Wu, L., Gray, R., Chhetri, D.K., 2020. Three-dimensional vocal fold structural change due to implant insertion in medialization laryngoplasty. PLoSOne 15 (1), e0228464.